J. Coat. Technol. Res., **12** (6) 1173–1183, 2015
DOI 10.1007/s11998-015-9715-y

Enhancing the stability of polystyrene ultrathin films by using star-shape polymers as dewetting inhibitors

Nampueng Pangpaiboon, Rakchart Traiphol, Nisanart Traiphol

Abstract This contribution introduces a new class of materials for improving the stability of polystyrene (PS) ultrathin films. Two types of three-arm polystyrenes (TA-PS) with different arm lengths are added into PS thin films with thicknesses of 7 and 23 nm. Concentration of the TA-PS additives is varied from 0 to 40 wt%. The morphological change of PS films upon annealing above its glass transition temperature is followed by utilizing optical and atomic force microscopy. Our results show that the addition of TA-PS into PS films leads to significant improvement of the film stability. The dewetting rate of PS film containing only 5 wt% of TA-PS is 3 times slower than that of the pure PS film. The increase of TA-PS concentration results in systematic decrease of the dewetting rate. We also observe that the dewetting-suppression efficiency of the TA-PS depends significantly on its arm length.

Keywords Coating, Polystyrene, Dewetting inhibition, Film stability

N. Pangpaiboon, N. Traiphol (✉)
Research Unit of Advanced Ceramics, Department of Materials Science, Faculty of Science, Chulalongkorn University, Bangkok 10330, Thailand
e-mail: nisanart.t@chula.ac.th

R. Traiphol
Laboratory of Advanced Polymers and Nanomaterials, Department of Chemistry and Center for Innovation in Chemistry, Faculty of Science, Naresuan University, Phitsanulok 65000, Thailand

R. Traiphol
NANOTEC-MU Excellence Center on Intelligent Materials and Systems, Faculty of Science, Rama 6 Road, Ratchathewi, Bangkok 10400, Thailand

Introduction

Polymeric thin films have numerous technological applications such as dielectric coating, lithography resisting, electronic packaging, and surfaces lubricating. As many electronic products and other devices are becoming smaller, the thinner polymeric coating is required. However, many ultrathin polymeric films have problems with instability as the films tend to break up and dewet the substrate surface. The issues must be addressed to obtain a homogenous and continuous coating. It has been known that the stability of polymeric thin films depends on many parameters such as film thickness, interfacial interactions, temperature, and molecular weight.[1–5] By decreasing film thickness and/or annealing above glass transition temperature (T_g), the polymeric films tend to become unstable and disintegrate into droplets.[1–3,6] This phenomenon is known as the dewetting, which can generally be described by three stages.[1,3,7] At an early stage, the increase of thermal interfacial fluctuation upon annealing above T_g causes the formation of small holes on the film. With an increase in the annealing time, the holes grow and eventually coalesce, forming unstable polygon structures. In the final stage, the polygons break up into hemispherical droplets where the interfacial energy determines their contact angles. Generally, the dewetting mechanisms can occur via spinodal and/or heterogeneous nucleation processes. Detailed descriptions of polymeric film dewetting are available in the literature.[1,3] An unfavorable interfacial interaction between polymeric molecules and the solid substrate accelerates the dewetting process.[7]

Scientists have made tremendous efforts, seeking the effective methods to eliminate or at least retard the dewetting of polymeric thin films. The techniques used for inhibiting this behavior are based on two general principles, thermodynamics and kinetics.[7] The thermodynamic strategy focuses on surface energies of solid

substrate and/or polymeric molecules. By modifying the interfacial tension between film and substrate, the stability of polymeric thin film is improved.[8–20] For example, the substrate surface is modified by chemical compositions with high affinity to the polymer film.[10] Thus, the interfacial tension between film and substrate is attuned, which improves the stability of polymeric thin film. Although the substrate modification can provide strong interfacial interactions, it generally involves a complicated process. An alternative technique relies on polymer modification. Functionalized polymers with adherent groups can segregate to the solid substrate.[11–16,18,19,21] Therefore, the addition of functionalized polymers such as sulfonated polystyrene with a sulfonation level of 0.76-6.5 mol% or poly(styrene-*stat*-chloromethylstyrene) with 5 mol% of chloromethylstyrene group into polystyrene (PS) thin film can enhance interfacial interactions, which in turn retard the dewetting process.[12,13,15,16] A fascinating strategy to suppress the dewetting of polymeric thin films is also presented by Barnes et al.[22] The addition of small amounts of fullerene nanoparticles into PS and polybutadiene thin films results in significant enhancement of their stability. In recent years, many researchers have investigated the mechanism of this phenomenon and have discovered that other nanoparticles can also be used as dewetting inhibitors.[23–33]

The suppression of thin film dewetting can also be achieved by reducing the mobility of polymeric chains. This technique is based on kinetic strategy. The addition of chemical crosslinkers or some foreign molecules to polymeric films promotes interchain interactions, which in turn results in the increase of film viscosity (i.e., decrease of polymer mobility). The chemical crosslinking can be generated by UV-light irradiation or the addition of some chemical agents.[34] The improvement of thin film stability by adding foreign molecules is rarely investigated. Xu and co-workers investigated the dewetting process of blended films between linear PS and four-arm poly(4-vinylbenzyl chloride) (PVBC).[35] Since the surface energy of four-arm PVBC is relatively high, they segregate to polar SiO_x/Si substrate, forming a bilayer structure. The improved interfacial interaction in this system leads to the increase of film stability. Our recent study proposes a new class of highly branched aromatic (HBA) molecules as a dewetting inhibitor for PS thin films.[36] We observe that the addition of only 0.5 wt% HBA results in a significant increase of the PS film stability.

In this study, we present our continuous efforts to explore a different class of materials as a dewetting inhibitor for PS thin films. Two types of three-arm polystyrene (TA-PS) are added into PS thin films with thicknesses of about 7 and 23 nm. The chemical structure of TA-PS with different arm lengths is shown in Fig. 1a. The surface energy of TA-PS is comparable to that of PS (see Table 1). Therefore, TA-PS molecules are expected to randomly disperse within the PS matrix (see Fig. 1b). Chain entanglement between the added PS arms and PS matrix should reduce the chain mobility, resulting in the increase of film stability. We investigate different structural and experimental parameters including the arm length of TA-PS, molecular weight of PS, and film thickness.

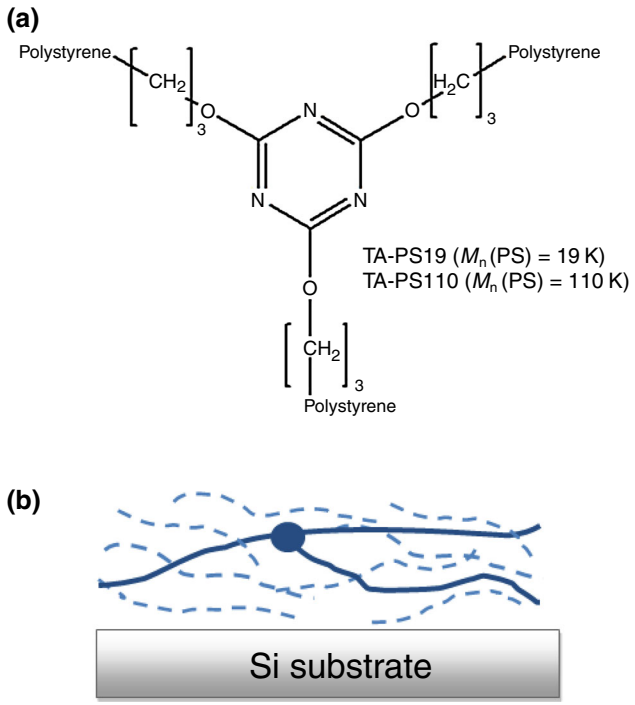

Fig. 1: (a) Chemical structures of TA-PS19, TA-PS110, and (b) the illustration of TA-PS molecules in PS film coated on SiOx/Si substrate. The arms of TA-PS interact with PS chains (dashed lines)

Table 1: M_n, M_w/M_n, and T_g of PS and three-arm PS

Polymer	M_n (g/mol)	M_w/M_n	T_g (°C)
PS11K	11,000	1.05	93
PS33K	33,000	1.04	103
TA-PS19	18,900 (of each arm)	1.09	106
TA-PS110	109,800 (of each arm)	1.09	106

Experimental

PS with narrow size distribution (PS11K and PS33K) and two types of three-arm PS (TA-PS19 and TA-PS110) were purchased from Polymer Source Inc. (Canada). Table 1 lists M_n, M_w/M_n, and T_g of all polymers used in this study. The M_n and M_w/M_n were provided by the supplier, while the T_g was measured by differential scanning calorimetry (DSC) technique.[11] Solutions of mixed PS and TA-PS were prepared in toluene (AR grade). The concentrations of TA-PS were 0, 2, 5, 10, 20, and 40 wt%. These solutions were clear and stable, indicating the miscibility of the two

Table 2: Contact angles of water and diiodomethane on different surfaces and their solid surface tension components calculated using a simultaneous equation of the Owens–Wendt–Kaelble approach[37]

Type of surfaces	θ_{water}	$\theta_{diiodomethane}$	γ_S^d (mJ/m^2)	γ_S^h (mJ/m^2)	γ_S (mJ/m^2)
Silicon	46 ± 1	39 ± 1	39.6 ± 0.6	20.6 ± 0.3	60.2 ± 0.9
Polystyrene	94 ± 2	21 ± 2	46.8 ± 0.5	0.1 ± 0.1	46.9 ± 0.6
TA-PS19	92 ± 2	23 ± 2	46.0 ± 0.7	0.2 ± 0.1	46.2 ± 0.8
TA-PS110	91 ± 2	24 ± 2	45.7 ± 0.6	0.3 ± 0.2	46.0 ± 0.8

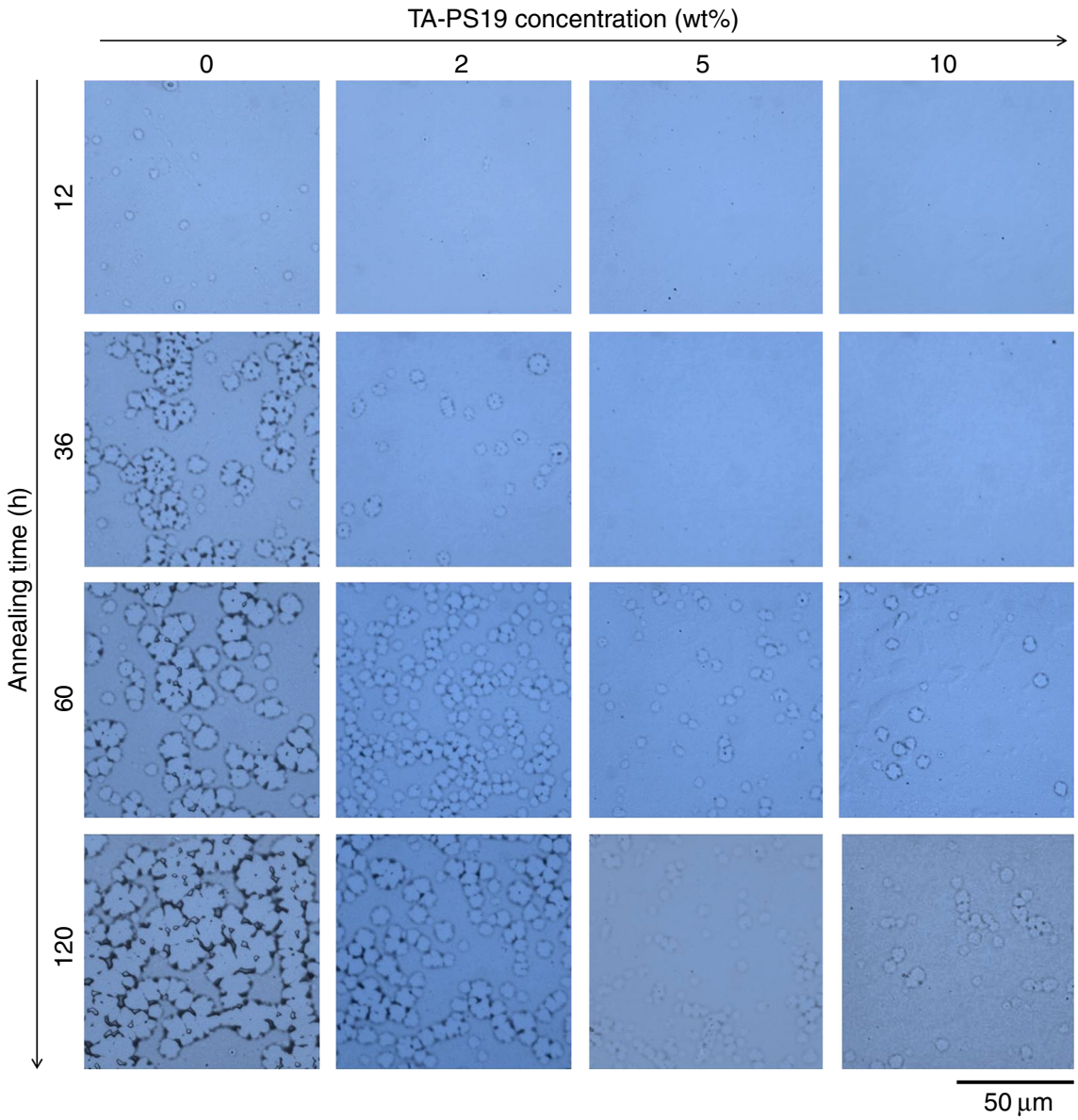

Fig. 2: Optical micrographs of 23-nm-thick PS11K films containing different concentrations of TA-PS19 annealed at 120°C for 12, 36, 60, and 120 h. Size of each image is 100 μm × 100 μm

components at room temperature. Viscosity of the solutions was measured using a Brookfield RVDV-E viscometer (Brookfield Engineering Laboratories, Inc.) with a small sample size adapter. Addition of TA-PS at 0–40 wt% did not affect the viscosity of solutions. The solutions remained clear with

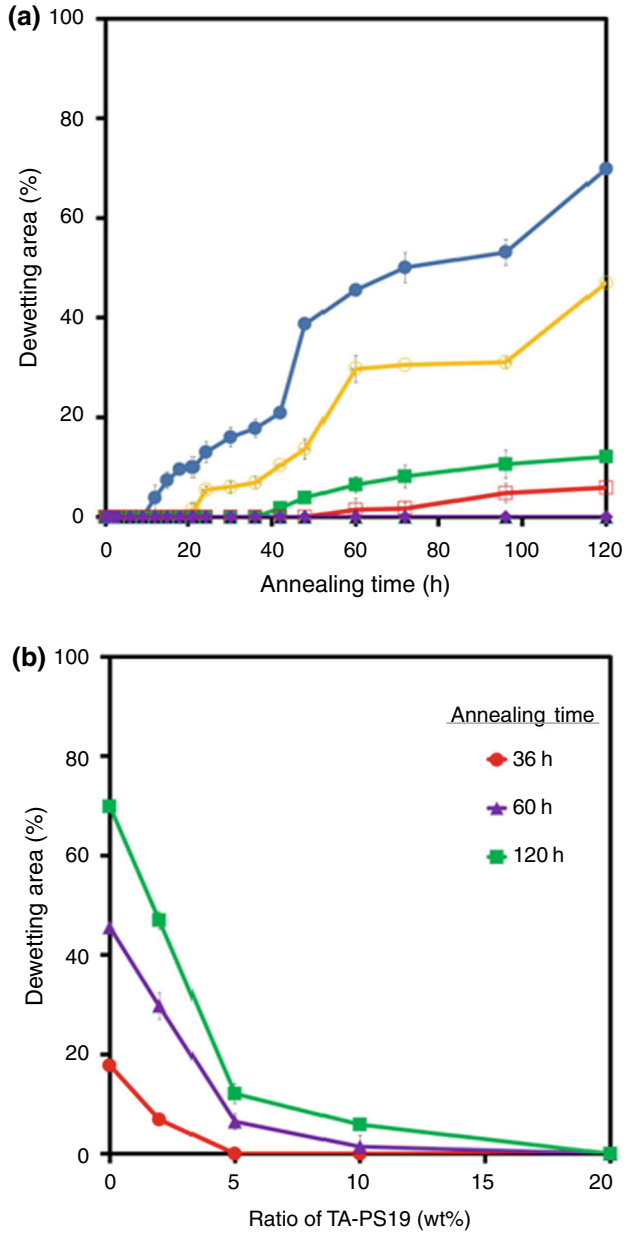

Fig. 3: (a) Dewetting area vs annealing time of 23-nm-thick PS11K films annealed at 120°C. Concentrations of TA-PS19 are (●) 0 wt%, (○) 2 wt%, (■) 5 wt%, (□) 10 wt%, (▲) 20 wt%, (Δ) 40 wt%, and (♦) 100 wt%. (b) Dewetting area of PS11K/TA-PS19 films vs ratio of TA-PS19

unchanged viscosity for 14 days under ambient conditions (results not shown).

Silicon wafers (SiO_x/Si) used as a substrate in these experiments were cleaned by a well-known method. The wafers were soaked in a 7:3 v/v solution of conc. H_2SO_4 and 30% H_2O_2 at about 80°C for 1 h. The substrates were rinsed with deionized water several times and dried by pressurized nitrogen gas. Freshly cleaned substrates were used for the preparation of polymeric thin films. Since all substrates were cleaned by using the same conditions, chemical compositions on the substrate surface were expected to be the same. Thin films of PS on SiO_x/Si were prepared by spin casting from 0.1 and 0.3 wt% solutions, yielding thicknesses of about 7 and 23 nm, respectively. The spinning rate was kept constant at 1000 rpm for 10 s. Three samples were prepared for each condition. The film thickness was measured by ellipsometry (Gaertner Scientific Corporation). We also measured the depth of holes detected in those films by using atomic force microscopy (AFM). The results are consistent with their thicknesses. Since the viscosities of solutions with various TA-PS concentrations were similar, the resulting films exhibited comparable thickness. Surface energies of PS, three-arm PS, and SiO_x/Si were measured following the Owens–Wendt–Kaelble approach, described in our previous reports.[15,36,37] Water and diiodomethane were used as solvents. Static contact angles of the solvent droplets on each surface were measured by using a goniometer (CAM-PLUS Tantec, U.S. Patent, USA). The amount of the solvents in the droplets was controlled to be the same by using a syringe. Averaged values of contact angles obtained from at least 5 measurements were used in the calculation of surface energies. The obtained results are listed in Table 2.

The dewetting of PS thin films was induced by annealing the samples in a vacuum oven at 115, 120, and 165°C depending on their thicknesses. The annealed films were periodically quenched to room temperature by placing on a metal surface. Global structure of the films at different annealing time was investigated using optical microscopy (OM, Olympus PX 60 M equipped with digital camera Olympus model DP12). OM images were recorded under reflectance mode with the magnification of ×100, ×200, ×500, and ×1000. Holes appeared as the lighter area compared to the coated polymer film. The dewetted areas (holes) were verified by using AFM. The evolution of local structure upon the annealing was followed by AFM (SPI3800N Nanoscope II, Seiko Instrument Inc., Japan) operating in a dynamic contact mode. The spring constant of the cantilever was about 20 N/m. The AFM measurements were performed under ambient conditions. Scan sizes were varied from about 20×20 to 1×1 μm^2. The dewetting areas were measured by using commercial graphical analysis software. We set the cut-off value for the brightness of domains within the optical image. This cut-off value is set to equal that of the coated area. The areas with brightness higher than this cut-off value correspond to the dewetted areas. Therefore, the software can calculate the dewetted area with respect to the total area.

Results and discussion

Effects of TA-PS additive on film stability

In the first section, we investigate the ability of TA-PS as a dewetting inhibitor of PS film. PS11K and TA-

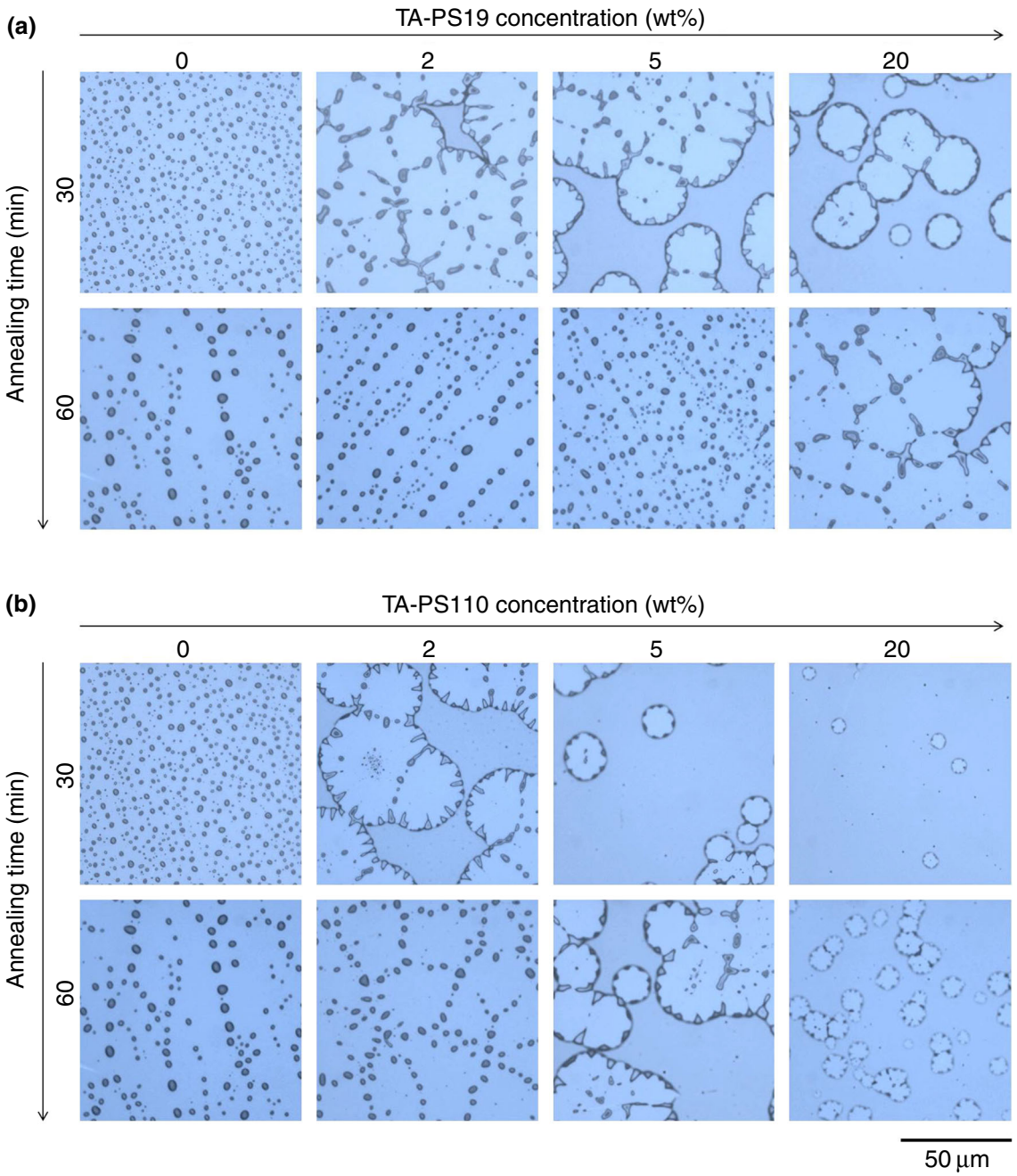

Fig. 4: Optical micrographs of 23-nm-thick PS33K films containing different concentrations of (a) TA-PS19 and (b) TA-PS110 annealed at 165°C for 30 and 60 min. Size of each image is 100 μm x 100 μm

PS19 are used as a polymer matrix and an additive, respectively. Since the entanglements of PS chains occur at molecular weight above 18 K,[38,39] the PS11K film behaves as a simple liquid in the melt state. Molecular weight of PS arm (19 K) is just above the threshold value required for the chain entanglement. This allows us to observe the clear effects of TA-PS19 on the film stability. The concentrations of TA-PS19 in 23-nm-thick PS11K films are increased from 0 to 40 wt%. All films are annealed at the same time in a vacuum oven to minimize experimental errors. The annealing of pure PS11K thin films at 120°C, which is above its glass transition temperature (T_g),[11] for 12 h induces the formation of small holes as shown in Fig. 2. The observation of these holes corresponds to an early stage of the film dewetting.[3] All of the blended PS11K/TA-PS19 films, however, still completely spread over the substrate at this condition. When the annealing time is increased above 22 h, some small holes are observed in the film containing 2 wt% of TA-PS19.

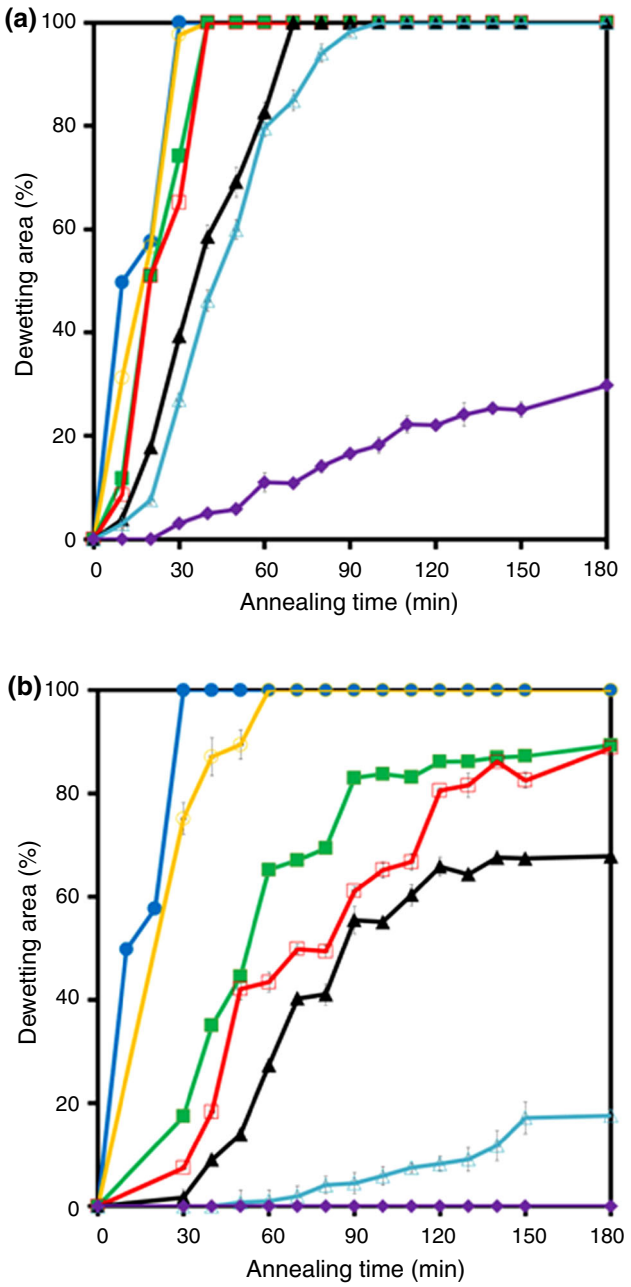

Fig. 5: Dewetting area vs annealing time of 23-nm-thick PS33K films annealed at 165°C. Concentrations of (a) TA-PS19 and (b) TA-PS110 are (●) 0 wt%, (○) 2 wt%, (■) 5 wt%, (□) 10 wt%, (▲) 20 wt%, (Δ) 40 wt%, and (♦) 100 wt%

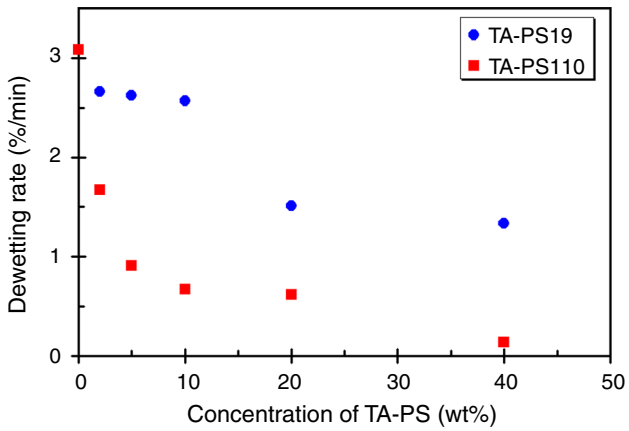

Fig. 6: Dewetting rate of PS33K/TA-PS19 films and PS33K/TA-PS110 films

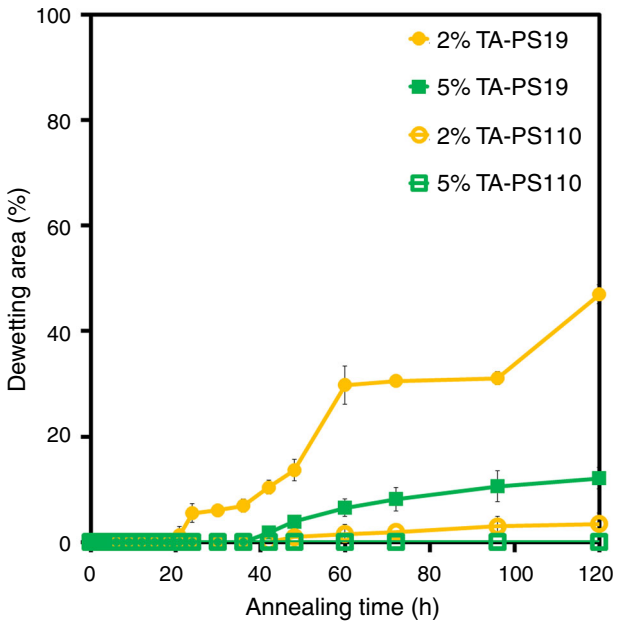

Fig. 7: Dewetting area vs annealing time of 23-nm-thick PS11K films annealed at 120°C. Concentrations of TA-PS19 and TA-PS110 are 2 and 5 wt%

This result indicates that the dewetting process of this blended film is much slower than that of the pure PS11K film. The increase of TA-PS19 concentration to 5, 10, 20, and 40 wt% results in a systematic decrease of the dewetting rate. The small holes start to form at about 42 and 60 h in the blended films containing 5 and 10 wt% of TA-PS19, respectively. For the blended films with TA-PS19 concentrations of 20 and 40 wt%, the increase of annealing time to 120 h still does not induce the formation of any hole. Our results show that the addition of TA-PS19 into PS11K thin films leads to drastic increase of their stability.

The dewetting behaviors of all films are compared in Fig. 3a, where the dewetting area is plotted as a function of annealing time. The dewetting rates of each system are described by the slopes of these plots. It is obvious that the dewetting rate systematically decreases upon increasing concentration of the TA-PS19. The plots in Fig. 3b show systematic decrease of the dewetting area with increasing TA-PS19 concentration. At annealing time of 120 h, the dewetting area is about 70%, 47%, 12%, 6%, and 0% for the PS films

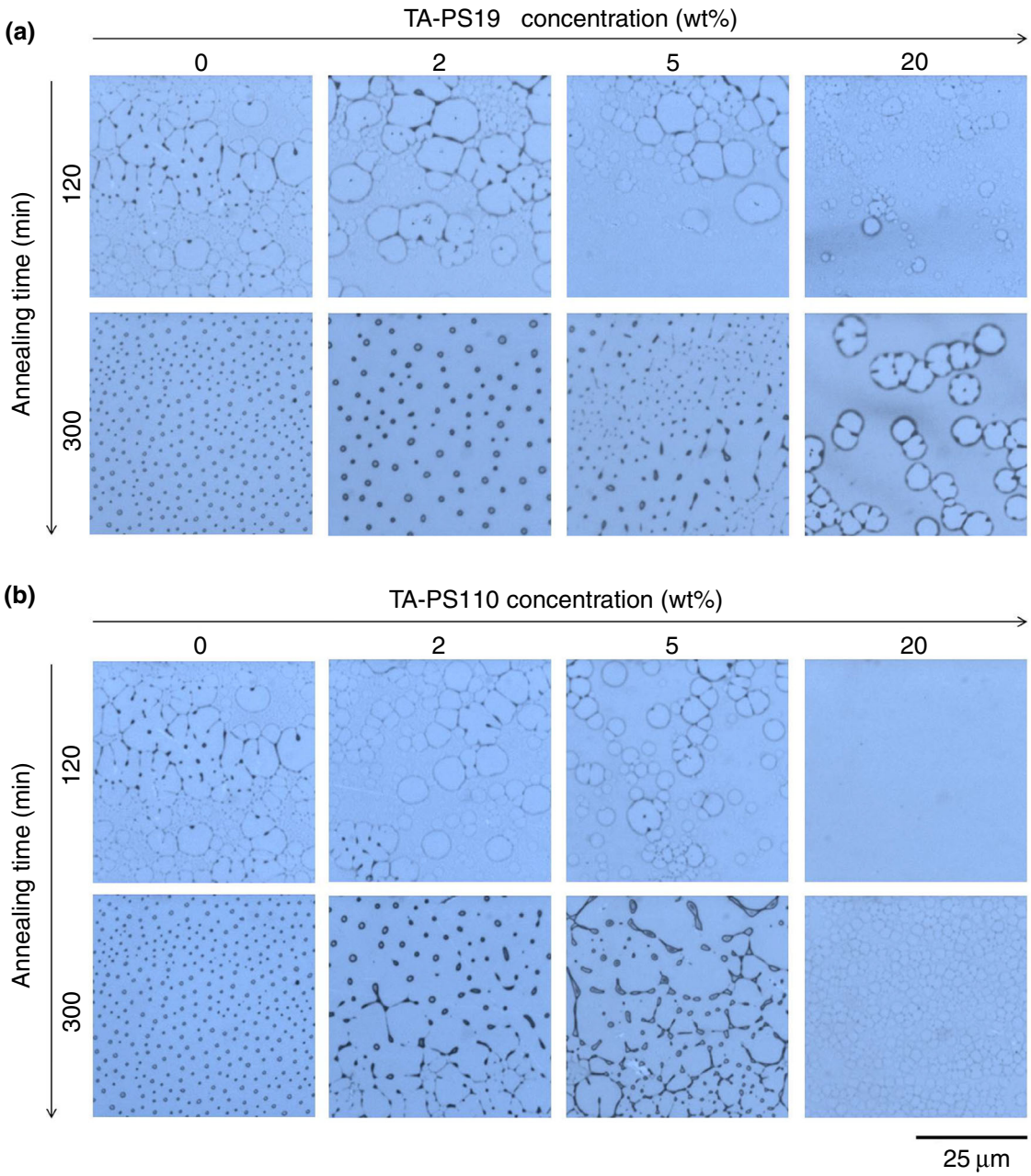

Fig. 8: Optical micrographs of 7-nm-thick PS33K films containing different concentrations of (a) TA-PS19 and (b) TA-PS110 annealed at 115°C for 120 and 300 min. Size of each image is 50 μm x 50 μm

containing 0, 2, 5, 10, and 20 wt% of TA-PS19, respectively. These results indicate that the TA-PS19 molecule behaves as a dewetting inhibitor of PS11K film. The surface energy of TA-PS19 is comparable to that of PS as shown in Table 2. Therefore, the TA-PS19 molecules are expected to randomly distribute within the film where the PS arms of TA-PS19 entangle with PS matrix. We suggest that the increase of chain entanglement reduces the mobility of PS chains within the film. The dewetting rate systematically decreases with the increasing TA-PS19 concentration.

Effects of TA-PS arm length

This section investigates the influence of molecular weight of TA-PS on its efficiency as a dewetting inhibitor of PS film. Two types of TA-PS, TA-PS19 and TA-PS110, with different PS arm lengths, are used as additives for 23-nm-thick PS33K films. All the as-cast films at room temperature are continuous and exhibit a smooth surface. The PS33K film has a higher degree of chain entanglement (i.e., higher viscosity) compared to that of the PS11K film.[38,39] The dewetting rate of

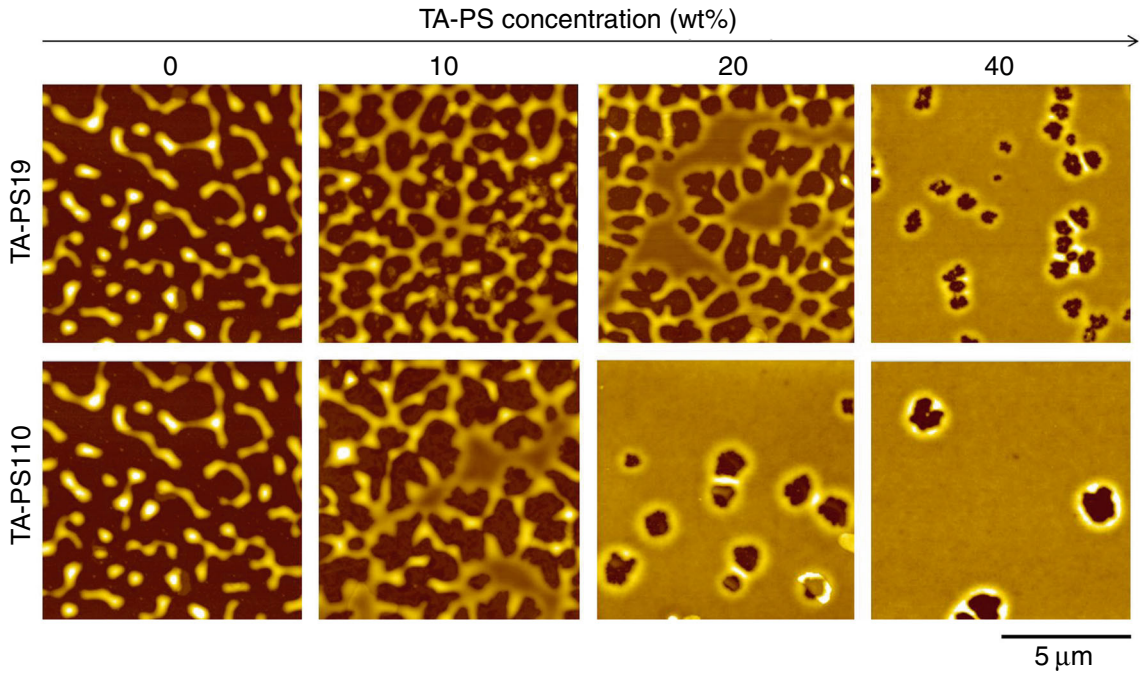

Fig. 9: AFM topography images of 7-nm-thick PS33K films containing different concentrations of TA-PS19 and TA-PS110 annealed at 115°C for 300 min. Sizes of the images are 10 μm x 10 μm

PS33K film is quite slow at 120°C. Therefore, the annealing temperature is increased to 165°C. Representative optical micrographs of PS33K films containing different concentrations of TA-PS19 and TA-PS110 are shown in Fig. 4. At this annealing condition, total dewetting of pure PS33K film is reached within 30 min where the continuous film breaks into polymer droplets. The addition of TA-PS19 and TA-PS110 into the PS33K film results in systematic decrease of the dewetting rate, consistent with the system of PS11K film. Figure 4 clearly shows that the dewetting area decreases with the increasing TA-PS concentration. Interestingly, the dewetting rate of blended PS33K/TA-PS films also depends on the arm length of TA-PS. The PS33K film containing 5 wt% of TA-PS19 reaches the final stage of dewetting within 40 min while a large fraction of the blended PS33K/TA-PS110 films remains coated on the substrate. A similar trend is observed in the PS33K films containing 10, 20, and 40 wt% of the TA-PS. This observation indicates that the dewetting rates of PS33K/TA-PS110 films are slower than those of the PS33K/TA-PS19 system. Therefore, the increase of TA-PS arm length promotes its efficiency as a dewetting inhibitor of PS film.

The dewetting rates of blended PS33K/TA-PS19 and PS33K/TA-PS110 films can be calculated from slopes of the plots in Fig. 5. The obtained results are summarized in Fig. 6. It is clear that the dewetting rate systematically decreases upon increasing the TA-PS concentration. The decrease of the dewetting rate also depends significantly on the arm length of TA-PS. The dewetting rate of pure PS33K is about 3.1%/min. It drops to 1.5 and 1.3%/min in the films containing 20 and 40 wt% of TA-PS19, respectively. It requires a much lesser amount of TA-PS110 to suppress the dewetting of PS33K films. The addition of only 2 wt% TA-PS110 reduces the dewetting rate to 1.7%/min. This comparison indicates that the dewetting-suppression efficiency of 2 wt% TA-PS110 is comparable to that of the 20 wt% TA-PS19. The increase of TA-PS110 concentration to 40 wt% causes the dewetting rate to drop to 0.13%/min, which is about 10 times less than that of the PS33K/TA-PS19 system. It is worthwhile to note that the pure TA-PS19 film still exhibits the higher dewetting rate (0.19%/min).

The investigation of the PS11K system provides similar results as shown in Fig. 7. Annealing the PS11K film containing 2 wt% TA-PS19 at 120°C for 120 h causes the increase of the dewetting area to about 45%. At the same experimental conditions, the dewetting area of blended PS11K/TA-PS110 film is only 3.4%. Our results indicate that the efficiency of TA-PS as a dewetting inhibitor can be promoted by increasing its arm length. We believe that the longer PS arm causes a higher degree of chain entanglement with PS matrix, which in turn results in better film stability.

Effects of film thickness

The previous works by our group observed that the effects of some foreign molecules on the film stability depend on film thickness.[15] The use of the same additives may lead to opposite results, depending on

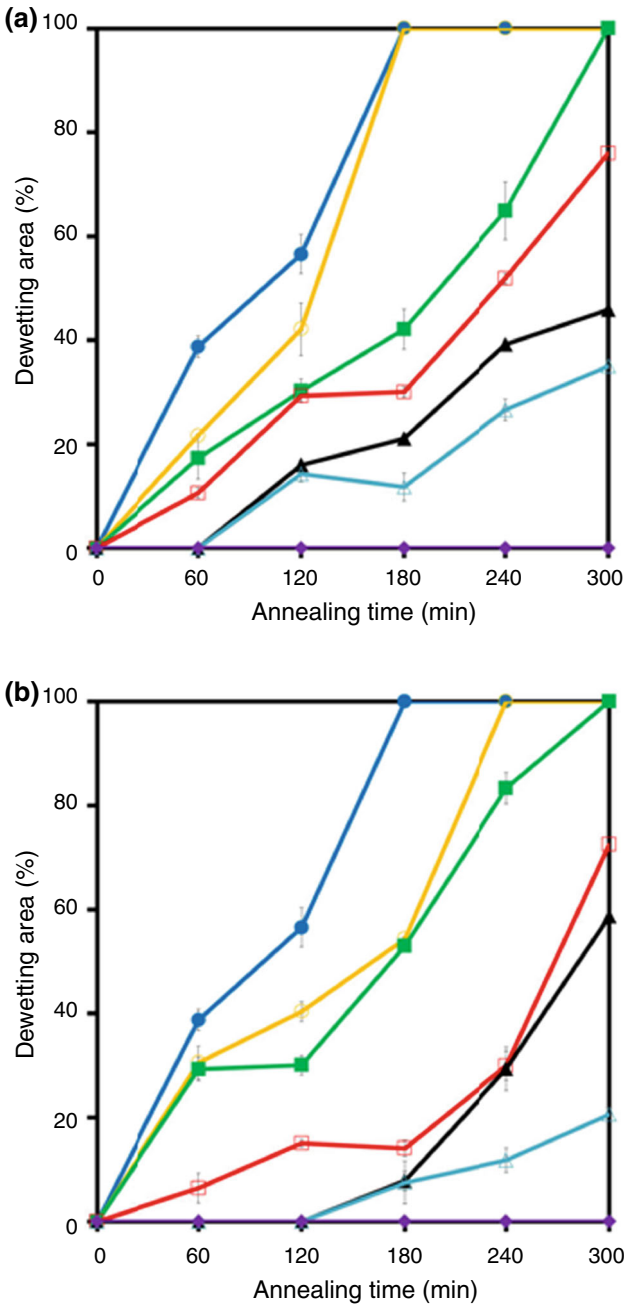

Fig. 10: Dewetting area vs annealing time of 7-nm-thick PS33K films annealed at 115°C. Concentrations of (a) TA-PS19 and (b) TA-PS110 are (●) 0 wt%, (○) 2 wt%, (■) 5 wt%, (□) 10 wt%, (▲) 20 wt%, (Δ) 40 wt%, and (♦) 100 wt%

the strength of polymer–polymer interactions and interfacial interactions with a solid substrate. Generally, the effect of interfacial interactions plays a significant role in the stability of ultrathin films.[1,2,7] The degree of chain entanglement, on the other hand, diminishes upon decreasing the film thickness.[40] In relatively thick film, the effect of chain entanglement and other types of interchain interactions becomes a dominant factor. To further explore the efficiency of TA-PS as a dewetting inhibitor, we investigate the dewetting behaviors of PS33K films with a thickness of ~7 nm. The films contain different amounts of TA-PS19 and TA-PS110, ranging from 0 to 40 wt%. The AFM measurements show that all the as-cast films are homogeneous and continuous. Annealing the pure PS33K film at 115°C for 120 min causes the formation of many holes as shown in Fig. 8. We observe that the dimension and number of holes systematically decrease with the increasing concentration of TA-PS19 and TA-PS110. The further increase of annealing time to 300 min causes total dewetting of pure PS33K film. The films containing 20 wt% of TA-PS19 and TA-PS110, however, partially dewet the substrate at the same annealing conditions. Our results show that the addition of TA-PS19 and TA-PS110 can still improve the stability of the 7-nm-thick PS33K films. AFM topography images in Fig. 9 confirm that local structures of the films containing 10, 20, and 40 wt% of TA-PS are consistent with global structures observed by optical microscopy. Moreover, probing local structure by the AFM in phase mode does not detect any phase separation in these systems. The dewetting area systematically decreases with the increasing TA-PS concentration. The holes detected in all films show the same morphology. Since the hole distributions in annealed films are random, the dewetting process is likely to occur via heterogeneous nucleation mechanism.[1,7]

The dewetting area as a function of annealing time of PS33K/TA-PS19 and TA-PS33K/PS110 films is shown in Fig. 10. The pure PS33K film exhibits the highest slope, indicating the highest dewetting rate (0.53%/min). The dewetting area reaches 100% at 180 min of annealing time. The dewetting rate drops to 0.24 and 0.12%/min in the films containing 10 and 40 wt% of TA-PS19, respectively. The PS33K/TA-PS110 system shows a larger drop of the dewetting rate. The presence of 10 and 40 wt% TA-PS110 causes the decrease of the dewetting rate to 0.21 and 0.07%/min, respectively. Therefore, the TA-PS110 is a more effective dewetting inhibitor consistent with the results in the previous section. Our results in this section show that the ability of TA-PS to suppress the dewetting of PS film still persists upon decreasing the film thickness to 7 nm.

Conclusions

We demonstrate that the star-shape polymers, TA-PS, can be utilized for suppression of the dewetting dynamics of PS ultrathin films. The addition of TA-PS molecules into PS thin films with thicknesses of 23 and 7 nm results in a significant decrease of the dewetting rate. We suggest that the TA-PS molecules enhance the chain entanglement within PS film. The arms of TA-PS entangle with the polymer matrix. The increase of arm length promotes the dewetting-sup-

pression efficiency of the TA-PS. Our results provide fundamental knowledge and a new method for improving stability of ultrathin polymeric film.

Acknowledgments This research is financially supported by the National Nanotechnology Center (NANOTEC), the National Science and Technology Development Agency (NTSDA) (Project P-10-10589). N. Pangpaiboon thanks the Office of the Higher Education Commission for supporting her Ph.D. scholarship under the program Strategic Scholarships for Frontier Research Network. This research is partially supported by the National Center of Excellence for Petroleum, Petrochemical, and Advanced Materials and the NANOTEC-MU Excellence Center on Intelligent Materials and Systems.

References

1. Geoghegan, M, Krausch, G, ''Wetting at Polymer Surface and Interfaces.'' *Prog. Polym. Sci.*, **28** 261–302 (2003)
2. Bucknall, DG, ''Influence of Interfaces on Thin Polymer Film Behavior.'' *Prog. Mater. Sci.*, **49** 713–786 (2004)
3. Reiter, G, ''Unstable Thin Polymer Films: Rupture and Dewetting Processes.'' *Langmuir*, **9** 1344–1351 (1993)
4. Reiter, G, ''Probing Properties of Polymers in Thin Films via Dewetting.'' *Adv. Polym. Sci.*, **252** 29–64 (2013)
5. Meredith, JC, Smith, AP, Karim, A, Amis, EJ, ''Combinatorial Materials Science for Polymer Thin-Film Dewetting.'' *Macromolecules*, **33** 9747–9756 (2000)
6. Shull, KR, Karis, TE, ''Dewetting Dynamics for Large Equilibrium Contact Angles.'' *Langmuir*, **10** 334–339 (1994)
7. Xue, L, Han, Y, ''Inhibition of Dewetting of Thin Polymer Films.'' *Prog. Mater. Sci.*, **57** 947–979 (2012)
8. Yuan, C, Ouyang, M, Koberstein, JT, ''Effects of Low-Energy End Groups on the Dewetting Dynamics of Poly(styrene) Films on Poly(methyl methacrylate) Substrates.'' *Macromolecules*, **32** 2329–2333 (1999)
9. Ashley, KM, Raghavan, D, Douglas, JF, Karim, A, ''Wetting-Dewetting Transition Line in Thin Polymer Films.'' *Langmuir*, **21** 9518–9523 (2005)
10. Choi, S-H, Zhang Newby, B-M, ''Suppress Polystyrene Thin Film Dewetting by Modifying Substrate Surface with Aminopropyltriethoxysilane.'' *Surf. Sci.*, **600** 1391–1404 (2006)
11. Traiphol, R, ''Influences of Chain Heterogeneity on Instability of Polymeric Thin Films: Dewetting of Polystyrenes, Polychloromethylstyrenes and its Copolymers.'' *J. Colloid Interface Sci.*, **310** 217–228 (2007)
12. Zhai, X, Weiss, RA, ''Wetting Behavior of Lightly Sulfonated Polystyrene Ionomers on Silica Surfaces.'' *Langmuir*, **24** 12928–12935 (2008)
13. Feng, Y, Karim, A, Weiss, RA, Douglas, JF, Han, CC, ''Control of Polystyrene Film Dewetting Through Sulfonation and Metal Complexation.'' *Macromolecules*, **31** 484–493 (1998)
14. Tucker, RT, Han, CC, Dobrynin, AV, Weiss, RA, ''Small-Angle Neutron Scattering Analysis of Blends with Very Strong Intermolecular Interactions: Polyamide/Ionomer Blends.'' *Macromolecules*, **36** 4404–4410 (2003)
15. Sangjan, S, Traiphol, N, Traiphol, R, ''Influences of Poly[(-styrene)$_x$-*stat*-(chloromethylstyrene)$_y$]s Additives on Dewetting Behaviors of Polystyrene Thin Films: Effects of Polar Group Ratio and Film Thickness.'' *Thin Solid Films*, **520** 4921–4928 (2012)
16. Sangjan, S, Traiphol, N, Traiphol, R, ''Improvement of Ultrathin Polystyrene Film Stability by Addition of Poly(styrene-*stat*-chloromethylstyrene) Copolymer: An Atomic Force Microscopy Study.'' *Thin Solid Films*, **518** 4879–4883 (2010)
17. Wunnicke, O, Müller-Buschbaum, P, Wolkenhauer, M, Lorenz-Haas, C, Cubitt, R, Leiner, V, Stamm, M, ''Stabilization of Thin Polymeric Bilayer Films on Top of Semiconductor Surfaces.'' *Langmuir*, **19** 8511–8520 (2003)
18. An, N, Li, Y, Yang, Y, Yu, F, Dong, L, ''Stabilization of Polymer Bilayers by Introducing Crosslinking at the Interface.'' *Macromol. Rapid Commun.*, **27** 955–960 (2006)
19. Miyamoto, K, Hosaka, N, Kobayashi, M, Otsuka, H, Yamada, N, Torikai, N, Takahara, A, ''Dewetting Inhibition and Interfacial Structures of Silsesquioxane-Terminated Polystyrene Thin Films.'' *Polym. J.*, **39** 1247–1252 (2007)
20. Han, X, Luo, C, Dai, Y, Liu, H, ''Effect of Polymer-Substrate Interactions on the Surface Morphology of Polymer Blend Thin Films.'' *J. Macro. Sci. Part B*, **47** 1050–1061 (2008)
21. Henn, G, Bucknall, DG, Stamm, M, Vanhoorne, P, Jérôme, R, ''Chain end Effects and Dewetting in Thin Polymer Films.'' *Macromolecules*, **29** 4305–4313 (1996)
22. Barnes, KA, Karim, A, Douglas, JF, Nakatani, AI, Gruell, H, Amis, EJ, ''Suppression of Dewetting in Nanoparticle-Filled Polymer Films.'' *Macromolecules*, **33** 4177–4185 (2000)
23. Pangpaiboon, N, Traiphol, N, ''Dewetting Suppression of Polystyrene Thin Film Using Titanium Dioxide Nanoparticles.'' *Key Eng. Mater.*, **608** 218–223 (2014)
24. Wengeler, L, Schmitt, M, Peters, K, Scharfer, P, Schabel, W, ''Comparison of Large Scale Coating Techniques for Organic and Hybrid Films in Polymer Based Solar Cells.'' *Chem. Eng. Process.*, **68** 38–44 (2013)
25. Mackay, ME, Hong, Y, Jeong, M, Hong, S, Russell, TP, Hawker, CJ, Vestberg, R, Douglas, JF, ''Influence of Dendrimer Additives on the Dewetting of Thin Polystyrene Films.'' *Langmuir*, **18** 1877–1882 (2002)
26. Besancon, BM, Green, PF, ''Polystyrene-Based Single-Walled Carbon Nanotube Nanocomposite Thin Films: Dynamics of Structural Instabilities.'' *Macromolecules*, **38** 110–115 (2004)
27. Krishnan, RS, Mackay, ME, Hawker, CJ, Van Horn, B, ''Influence of Molecular Architecture on the Dewetting of Thin Polystyrene Films.'' *Langmuir*, **21** 5770–5776 (2005)
28. Chung, H-J, Ohno, K, Fukuda, T, Composto, RJ, ''Internal Phase Separation Drives Dewetting in Polymer Blend and Nanocomposite Films.'' *Macromolecules*, **40** 384–388 (2006)
29. Kropka, JM, Green, PF, ''Control of Interfacial Instabilities in Thin Polymer Films with the Addition of a Miscible Component.'' *Macromolecules*, **39** 8758–8762 (2006)
30. Xavier, JH, Sharma, S, Seo, YS, Isseroff, R, Koga, T, White, H, Ulman, A, Shin, K, Satija, SK, Sokolov, J, Rafailovich, MH, ''Effect of Nanoscopic Fillers on Dewetting Dynamics.'' *Macromolecules*, **39** 2972–2980 (2006)
31. Gu, X, Chen, G, Zhao, M, Watson, SS, Nguyen, T, Chin, JW, Martin, JW, ''Critical Role of Particle/Polymer Interface in Photostability of Nano-filled Polymeric Coatings.'' *J. Coat. Technol. Res.*, **9** 251–267 (2012)
32. Hosaka, N, Otsuka, H, Hino, M, Takahara, A, ''Control of Dispersion State of Silsesquioxane Nanofillers for Stabilization of Polystyrene Thin Films.'' *Langmuir*, **24** 5766–5772 (2008)
33. Mukherjee, R, Das, S, Das, A, Sharma, SK, Raychaudhuri, AK, Sharma, A, ''Stability and Dewetting of Metal Nanoparticle Filled Thin Polymer Films: Control of Instability Length Scale and Dynamics.'' *ACS Nano*, **4** 3709–3724 (2010)
34. Carroll, GT, Sojka, ME, Lei, X, Turro, NJ, Koberstein, JT, ''Photoactive Additives for Cross-Linking Polymer Films: Inhibition of Dewetting in Thin Polymer Films.'' *Langmuir*, **22** 7748–7754 (2006)

35. Xu, L, Yu, X, Shi, T, An, L, ''Dewetting of Linear Polymer/Star Polymer Blend Film.'' *Macromolecules*, **41** 21–24 (2007)
36. Pangpaiboon, N, Traiphol, N, Promarak, V, Traiphol, R, ''Retardation the Dewetting Dynamics of Ultrathin Polystyrene Films Using Highly Branched Aromatic Molecules as Additives.'' *Thin Solid Films*, **548** 323–330 (2013)
37. Kwok, DY, Neumann, AW, ''Contact Angle Measurement and Contact Angle Interpretation.'' *Adv. Colloid Interface Sci.*, **81** 167–249 (1999)
38. Montfort, J-P, Marin, G, Monge, P, ''Effects of Constraint Release on the Dynamics of Entangled Linear Polymer Melts.'' *Macromolecules*, **17** 1551–1560 (1984)
39. Watanabe, H, Sakamoto, T, Kotaka, T, ''Entanglements in Linear Polystyrenes.'' *Macromolecules*, **18** 1436–1442 (1985)
40. Brown, HR, Russell, TP, ''Entanglements at Polymer Surfaces and Interfaces.'' *Macromolecules*, **29** 798–800 (1996)